Available online at www.sciencedirect.com

ScienceDirect

www.elsevier.com/locate/jes

JES JOURNAL OF ENVIRONMENTAL SCIENCES

www.jesc.ac.cn

Effect of phosphate on heterogeneous Fenton oxidation of catechol by nano-Fe_3O_4: Inhibitor or stabilizer?

Xiaofang Yang[1,*,**], *Jie He*[1,2,**], *Zhongxi Sun*[3], *Allan Holmgren*[4], *Dongsheng Wang*[1,2,*]

1. *Research Center for Eco-Environmental Sciences, Chinese Academy of Sciences, Beijing 100085, China. E-mails: xfyang@rcees.ac.cn (Xiaofang Yang); hejie10@mails.ucas.ac.cn (Jie He),*
2. *University of Chinese Academy of Sciences, Beijing 100049, China*
3. *School of Chemistry and Chemical Engineering, University of Jinan, Jinan 250022, China*
4. *Chemical Engineering, Department of Civil, Environmental and Natural Resources Engineering, Luleå University of Technology, SE-971 87, Sweden*

ARTICLE INFO

Article history:
Received 28 July 2015
Revised 6 November 2015
Accepted 11 November 2015
Available online 21 December 2015

Keywords:
Heterogeneous Fenton oxidation
Adsorption
ATR-FTIR
Interface mechanism

ABSTRACT

The effect of phosphate on adsorption and oxidation of catechol, 1,2-dihydroxybenzene, in a heterogeneous Fenton system was investigated. *In situ* attenuated total reflectance infrared spectroscopy (ATR-FTIR) was used to monitor the surface speciation at the nano-Fe_3O_4 catalyst surface. The presence of phosphate decreased the removal rate of catechol and the abatement of dissolved organic compounds, as well as the decomposition of H_2O_2. This effect of phosphate was mainly due to its strong reaction with surface sites on the iron oxide catalyst. At neutral and acid pH, phosphate could displace the adsorbed catechol from the surface of catalyst and also could compete for surface sites with H_2O_2. *In situ* IR spectra indicated the formation of iron phosphate precipitation at the catalyst surface. The iron phosphate surface species may affect the amount of iron atoms taking part in the catalytic decomposition of H_2O_2 and formation of hydroxyl radicals, and inhibit the catalytic ability of Fe_3O_4 catalyst. Therefore, phosphate ions worked as stabilizer and inhibitor in a heterogeneous Fenton reaction at the same time, in effect leading to an increase in oxidation efficiency in this study. However, before use of phosphate as pH buffer or H_2O_2 stabilizer in a heterogeneous Fenton system, the possible inhibitory effect of phosphate on the actual removal of organic pollutants should be fully considered.

Introduction

The heterogeneous Fenton reaction, as one of the advanced oxidation processes (AOPs), has drawn extensive attention due to its unique advantages in the removal of organic pollutants from contaminated waters and soils (Pignatello et al., 2006; Li and Qu, 2009). Similar to the classic Fenton reaction, the heterogeneous Fenton reaction of a Fe-containing solid catalyst could generate hydroxyl radicals from H_2O_2 (Pignatello et al., 2006; Matta et al., 2008; Duan et al., 2014). The produced

* *Corresponding author E-mail: wgds@rcees.ac.cn (Dongsheng Wang).*
** These authors contributed equally to this work.

http://dx.doi.org/10.1016/j.jes.2015.11.007
1001-0742/

hydroxyl radicals have high ability and non-selectivity for oxidation of organic substances. However, the mechanism of H_2O_2 catalytic decomposition and organic oxidation initiated by the surface of the catalyst is still speculative, and the role of the surface is not clear.

It has been observed that the degradation of organics in the heterogeneous Fenton system is efficient at even near neutral pH, and the rate of reaction is surface mechanism controlled (Matta et al., 2008; Pham et al., 2009; Xue et al., 2009; Zhang et al., 2009). Many investigations have proved that the interface reaction of H_2O_2 on the catalyst is the essential step for the generation of hydroxyl radicals (Lin and Gurol, 1998; Xu and Wang, 2012; Nie et al., 2015). Accordingly, the heterogeneous Fenton oxidation of organics is much slower than the classic Fenton reaction, although a higher degree of mineralization can be accomplished by the heterogeneous reaction (Teel et al., 2001). One drawback for the heterogeneous Fenton oxidation process is the nonproductive decomposition of H_2O_2 into H_2O and O_2 (Lin and Gurol, 1998), which makes it less efficient and more expensive. Previous studies have found that some metal-complexing ligands, such as phosphate, silicate, and some polycarboxylates, could stabilize H_2O_2 against nonproductive decomposition (Watts et al., 1999, 2007; Pham et al., 2012). However, the effect of these ligands on organics removal has not been fully evaluated.

Phosphate, known as a strong ligand for iron oxide, is often used as a pH-buffer solution and also exists as a ubiquitous biogenic element in natural water. Therefore, the effect of phosphate on heterogeneous Fenton oxidation must be considered when it is used in water and wastewater treatment as well as in soil remediation. In the present study, catechol was chosen as a model organic pollutant, to explore the effect of phosphate on the oxidation and interface reaction in the heterogeneous Fenton oxidation process. The chemical reactions occurring at the nano-Fe_3O_4 catalyst surface were monitored by *in situ* attenuated total reflectance infrared spectroscopy (ATR-FTIR), to further elucidate the surface speciation and mechanism of the heterogeneous Fenton reaction.

1. Materials and methods

1.1. Chemicals and materials

Magnetite nanoparticles (MNPs) were synthesized by coprecipitation of Fe(II) and Fe(III) with 0.9 mol/L NH_4OH solution, based on the method described by Jolivet and Tronc (1988). Part of the synthesized magnetite was freeze-dried and stored in a desiccator under N_2 atmosphere for further characterization and batch experiments. The crystal structure of the synthesized magnetite was confirmed using powder X-ray diffraction (XRD) analysis (X'Pert PRO MPD, Panalytical, Netherland). The specific surface area of the synthesized magnetite measured by N_2-adsorption BET analysis was about 80 m^2/g, and the particle size was about 10 nm as measured from a scanning electron microscope (SEM) images (Appendix A Fig. S1). The point of zero charge (PZC) value of the synthesized magnetite particles in 0.01 mol/L NaCl solution was measured to be around 7.0.

Freshly prepared catechol (Merck) solution was used for oxidation and adsorption experiments. NaH_2PO_4 (Merck) was used to prepare a 0.050 mol/L aqueous phosphate stock solution. 30% (W/W) hydrogen peroxide solution (Merck) was used to initiate the heterogeneous Fenton reaction. NaOH and HCl solutions were used for pH adjustment. All chemical reagents were of analytical grade and used as received. All solutions were prepared using deoxygenated Milli-Q water.

1.2. Oxidation and adsorption experiments

Batch experiments were carried out in 50 mL polypropylene centrifuge tubes using 0.01 mol/L $NaNO_3$ solution as background electrolyte, and the experiments were performed in duplicate and at 25 ± 2 °C in a shaker in the dark. Catalytic oxidation experiments were carried out by addition of a certain amount of 30% H_2O_2 (W/W) after pre-adsorption of catechol on magnetite with or without phosphate. The suspensions were centrifuged and filtered through 0.22 μm syringe filters for analysis of the concentration of organics.

1.3. Analysis methods

The concentration of catechol was determined by high performance liquid chromatography (HPLC) with a UV Detector and a C18 column (5 μm, 250 mm × 4.6 mm). The mobile phase was water/acetonitrile (80:20, V/V) at pH 3 (adjusted with phosphoric acid), and the flow rate of mobile phase was set to 1.0 mL/min. The UV detector was operated at 275 nm. The concentration of H_2O_2 and phosphate was measured using the titanium sulfate method and ion chromatography (ICS-1500, Dionex, USA), respectively. The concentration of released Fe in solution before and after catalytic reaction was measured using inductively coupled plasma-optical emission spectroscopy (ICP-OES) (Optima 2000, PerkinElmer, USA). The reactive oxygen species (ROS) were identified by electron spin resonance (ESR) spectroscopy (ESP 300E, Bruker, Switzerland), operated at 3514 G center field and 9.85 GHz microwave frequency. The .OH was measured by using 5,5-Dimethyl-1-pyrroline-N-oxide (DMPO) as a spin trap agent.

1.4. ATR-FTIR measurements

The surface reaction of magnetite was monitored using the *in situ* flow-cell ATR-FTIR technique (Hug, 1997; Peak et al., 1999; Yang et al., 2008). The magnetite particles were deposited on one side of the ATR crystal by spreading the diluted magnetite dispersion on the crystal surface. The flow-cell ATR accessory consisted of a trapezoidal shaped ZnSe crystal (45°, 50 mm × 20 mm × 2 mm, 25-reflection total) and a 3 mL stainless steel flow-cell. Spectra were collected on a Bruker IFS 66v/s FTIR spectrometer equipped with a deuterated triglycine sulfate (DTGS) detector. All spectra were recorded by averaging 256 scans at a resolution of $4cm^{-1}$. A small amount of NaH_2PO_4 stock solution was added to the catechol solution before addition of H_2O_2. The reaction solution was argon gas purged and the pH was controlled with a pH-STAT Titrator (T70, Mettler Toledo, Swizerland) during the experiment. The reaction vessel and the tube for transferring solution to the flow-cell were

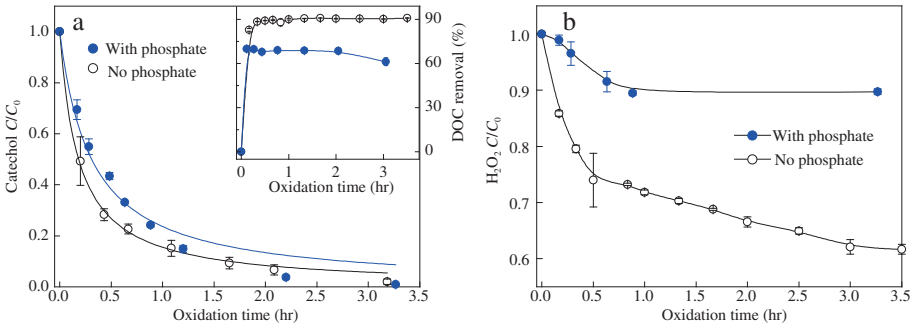

Fig. 1 – Effect of phosphate on (a) catechol removal and (b) H_2O_2 decomposition catalyzed by Fe_3O_4 nanoparticles (MNPs). $[Catechol]_0$ = 1 mmol/L, $[H_2O_2]_0$ = 0.05 mol/L, $[H_2PO_4^-]_0$ = 0.1 mmol/L, [MNPs] = 1 g/L, pH_0 = 6.5. Inset in (a): DOC removal.

wrapped with Al-foil to keep the solution from light. IR spectra were recorded at designated time intervals during the reaction. All experiments were performed at ambient temperature (22 ± 1 °C).

2. Results and discussion

2.1. *Effect of phosphate on catechol removal and H_2O_2 decomposition*

As shown in Fig. 1, the removal of catechol in the Fe_3O_4–H_2O_2 system was restrained by phosphate in the first 1 hr. However, almost all the catechol still could be removed after 3 hr despite the presence of phosphate. The experimental data in Fig. 1a could be fitted by a 2nd-order kinetic equation, and the fitted rate constant was 6.7 $(mmol/L)^{-1}\cdot hr^{-1}$ and 3.2 $(mmol/L)^{-1}\cdot hr^{-1}$ without and with phosphate respectively. The corresponding abatement of DOC decreased from 90% to 70% in the presence of phosphate, reflecting the reduction in the mineralization level of the heterogeneous Fenton oxidation process. The complete removal of the catechol parent compound may be attributed to its self-catalysis process through electron transfer between the generated quinones (DuVall and McCreery, 2000). Moreover, the decomposition of H_2O_2 was also inhibited significantly by phosphate (Fig. 1b). Only 10% of the initial H_2O_2 was decomposed in the presence of phosphate, compared to 40% of H_2O_2 was consumed without phosphate after 3 hr of reaction when catechol was completely removed.

It is well known that phosphate strongly adsorbs onto iron oxides and forms inner-sphere complexes at the surface (Persson et al., 1996). Watts et al. (1999) found that the decomposition rate of H_2O_2 decreased in the monobasic phosphate-stabilized goethite-H_2O_2 system compared with the unstabilized system, however the .OH production rate still increased as measured by the nitrobenzene removal method. Similarly, in the homogeneous Fenton reaction, the stability of H_2O_2 has also been found to be increased by phosphate, which was attributed to the inactivation of iron ions as catalyst, due to the complexation and precipitation of iron-phosphate species (Watts and Dilly, 1996; Pignatello et al., 2006). Accordingly, orthophosphate ($H_2PO_4^-$) was considered to be used as a H_2O_2 stabilizer in Fenton and Fenton-like reaction-based remediation of contaminated soils (Kakarla and Watts, 1997; Vicente et al., 2011). However, as revealed in the present work, the removal of catechol was reduced initially and the DOC removal was clearly inhibited in the presence of phosphate. Therefore, the use of phosphate as pH-buffering reagent or H_2O_2 stabilizer in the iron oxide-catalyzed heterogeneous Fenton process may generally reduce the mineralization of organic pollutants, although the consumption of H_2O_2 is significantly decreased. Therefore, the oxidation efficiency was calculated to quantitatively evaluate the effect of phosphate on organic removal by heterogeneous Fenton oxidation.

The oxidation efficiency E was calculated by Eq. (1) (Xue et al., 2009), where $\Delta[C_{catechol}]$ (mol/L) and $\Delta[H_2O_2]$ (mol/L) represent the concentration variation of catechol and H_2O_2 after 3 hr of oxidation. The E value increased from 0.052 to 0.198 in the presence of phosphate due to the reduced consumption of H_2O_2. Since almost all the catechol was eliminated after 3 hr of oxidation, the variation of DOC removal may better reveal the efficiency of oxidation and activity of the catalyst. Therefore, a modified oxidation efficiency value, mineralization efficiency E' (calculated as Eq. (2)) is proposed to evaluate the efficient utilization of H_2O_2 for organic pollutant removal.

$$E = \frac{\Delta[C_{catechol}]}{\Delta[H_2O_2]} \quad (1)$$

$$E' = \frac{\Delta[DOC]}{\Delta[H_2O_2]}. \quad (2)$$

In Eq. (2), Δ[DOC] (g/L) is the variation of DOC concentration and $\Delta[H_2O_2]$ (g/L) is H_2O_2 consumption. After 3 hr of oxidation, the E' of catechol in Fe_3O_4–H_2O_2 only increased from 0.11 to 0.29 in the presence of phosphate. Apparently, the oxidation efficiency and mineralization efficiency both increased when H_2O_2 consumption was inhibited.

Meanwhile, the concentration of phosphate in aqueous solution was rapidly decreased to 50% of the initial amount within the first hour of the oxidation reaction (Appendix A Fig. S2). After 1 hr of oxidation, the concentration of phosphate dropped and remained at *ca.* 0.05 mmol/L, which is closely consistent with the concentration variation of H_2O_2. The consumption of phosphate could have resulted from the sorption of phosphate on magnetite and possible reaction with radicals produced in the redox processes. Both of the

reactions would lead to an inhibitory effect on organic oxidation in the heterogeneous Fenton process. However, the reaction rate constant of phosphate with .OH was reported to be less than 2×10^4 $(mol/L)^{-1}$ sec^{-1} (Lipczynskakochany et al., 1995; Watts and Dilly, 1996), much lower than the rate constants for the reaction of .OH with organic molecules, which usually are in the range of 10^9 and 10^{10} $(mol/L)^{-1}$ sec^{-1}. Therefore, the sorption of phosphate contributed to the reduction in both the decomposition rate of H_2O_2 and removal efficiency of organics.

In the heterogeneous Fenton system, the interface reactions of organics, H_2O_2, possible ligands and H^+ with the catalyst are crucial to the decomposition of H_2O_2 and oxidation of organics (Xue et al., 2009; Hu et al., 2011; Xu and Wang, 2012), although the mutual interaction between these reactions is very difficult to precisely evaluate. Therefore, the competitive adsorption of catechol and phosphate on Fe_3O_4 and surface species changes during oxidation were carefully studied to reveal the effect and interface mechanism of phosphate on H_2O_2 decomposition and organic pollutant removal.

2.2. Adsorption of catechol and phosphate on Fe_3O_4

Fig. 2 shows the adsorption kinetic and isotherm curves of catechol on MNPs at pH 4.5, 6.5 and 8.0. The pseudo-2nd order kinetic equation $\left(\frac{t}{q_t} = \frac{1}{k_2 q_e^2} + \frac{t}{q_e}\right)$ could fit the kinetic experimental data well (Fig. 2a). The fitting parameters are listed in Appendix A Table S1. The kinetic results suggested that at least 90% of adsorption was accomplished within 1 hr at pH 8.0 and was favored at higher pH. At lower pH, the adsorption rate was reduced and about 65%–70% of the maximum amount of adsorption was achieved after 1 hr. The Langmuir adsorption equation $\left(q = \frac{q_m k_b c}{1 + k_b c}\right)$ could fit the isotherm experimental data well (Fig. 2b). Under the studied conditions, about 51% of catechol was removed from 0.2 mmol/L solution by adsorption at pH 8.0, while at pH 6.5 and 4.5 the corresponding adsorption amount of catechol was reduced to 40% and 38%, respectively. All the fitting results are summarized in Appendix A Table S1.

The adsorption of catechol increased with pH and initial concentration, which is consistent with the kinetic results and previous studies (Kummert and Stumm, 1980; Yang et al., 2012). However, there are also investigations showing that the amount of catechol adsorbed onto metal oxides, such as TiO_2 (PZC 6.5), Fe_2O_3 (PZC 6–7), MnO_2 (PZC 3) and Cr_2O_3 (PZC 6–9), is almost independent of pH in the pH range 3–8 and decreases at pH values larger than 8.5 for TiO_2 (Gulley-Stahl et al., 2010; Rodriguez et al., 2011). Fully protonated species (H_2Cat) are predominant in the catechol aqueous solution below pH 8.0 ($pK_{a1,catechol}$ = 9.2) (Martell and Smith, 1977), while the magnetite surface is positively charged in the acidic pH range and becomes negatively charged at pH > 7 (PZC). The negative charges of catechol species and magnetite surface both increase with pH. Therefore, the increased adsorption of catechol with pH observed in the present work precludes the electrostatic adsorption mechanism, indicating a chemical interaction between phenyl–hydroxyl groups of catechol and functional groups on the surface of magnetite particles. Moreover, an insignificant ionic strength effect on adsorption (Gulley-Stahl et al., 2010; Yang et al., 2012) further confirmed the inner-sphere surface complexation between catechol and oxide surface *via* ligand exchange or hydrogen-bonding.

By using the flow-cell ATR-FTIR technique, *in situ* IR spectra were recorded to acquire molecular information about the surface species formed on magnetite particles. Fig. 3 shows the ATR-FTIR spectra of catechol in solution and adsorbed onto magnetite at different pH values with and without phosphate. The spectral features of adsorbed catechol species (Fig. 3b) are different from the spectra of unsorbed species in solution (Fig. 3a). The spectra of adsorbed catechol were dominated by two peaks at 1480 and 1257 cm^{-1}, and the intensities of the two peaks decreased with pH, in accordance with the macroscopic experimental results that more catechol is adsorbed at higher pH. Compared with spectra of the $[Ti(Cat)_3]^{2-}$ complex (Lana-Villarreal et al., 2005), in which catecholate is known to chelate the central Ti(IV) ion to form a dianionic species, the similar spectral features in Fig. 3b indicated a similar structure of adsorbed catechol species. Moreover, the spectra in Fig. 3b are similar for adsorption spectra recorded at different pH values and catechol concentrations (data not shown), indicating a similar molecular configuration of adsorbed catechol species in the pH range 4.5–8.5 and different surface loadings. The frequencies and assignments of the spectral peaks are summarized in Table 1. Therefore, all these

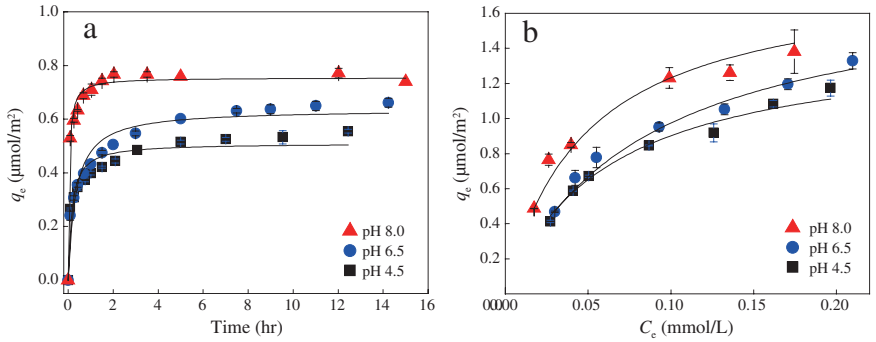

Fig. 2 – Adsorption kinetics (a) and adsorption isotherms (b) of catechol on MNPs at different pH. Solid lines in Figure (a) and (b) are pseudo-2nd order kinetic fitting and Langmuir fitting, respectively. $[catechol]_0$ = 0.1 mmol/L for kinetics experiments, $[nano\text{-}Fe_3O_4]_0$ = 1 g/L, $[NaNO_3]$ = 0.01 mol/L.

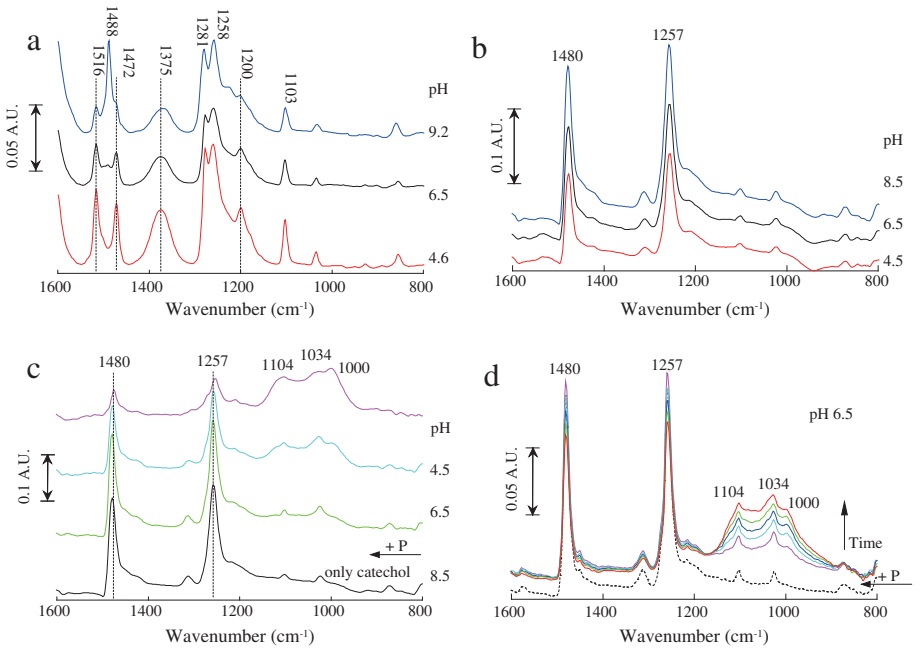

Fig. 3 – *In situ* attenuated total reflectance infrared spectroscopy (ATR-FTIR) spectra of (a) catechol solution, (b) catechol adsorption on Fe_3O_4, (c) competitive adsorption of catechol and phosphate at different pHs, (d) evolution of spectra upon addition of phosphate after pre-adsorption of catechol on Fe_3O_4 at pH 6.5. $[Catechol]_0$ = 0.2 mmol/L, $[Phosphate]_0$ = 0.05 mmol/L.

spectral changes upon adsorption of catechol onto magnetite strongly indicate the formation of chelates where catechol species were bound to the surface *via* a five-atom ring configuration with Fe atoms on the magnetite surface. However, a bidentate binuclear complex and minor contribution from a monodentate H-bonded structure cannot be excluded.

Table 1 – Peak position and assignments for infrared spectra of catechol in aqueous solution, catechol adsorbed on magnetite, and species adsorbed in Fenton-like reaction.

Catechol aqueous solution			Adsorbed catechol species			Fe_3O_4–H_2O_2 system			Assignment
H_2CAT		H_2CAT + $HCAT^-$	0.2 mmol/L			0.2 mmol/L	0.2 mmol/L + P	1 mmol/L	
pH 4.6	pH 6.5	pH 9.2	pH 4.5	pH 6.5	pH 8.5	pH 6.5	pH 6.5	pH 6.5	
								1601	ν(CC), δ(CH)
								1568	ν(CC), δ(CH)
						1532	1532	1532vs	ν(COO)
1516vs	1516s	1516						1503	ν(CC), δ(CH)
		1488vs	1480vs	1480vs	1480vs	1487vs	1485vs	1484	ν(CC)
1472s	1472	1472sh				1457sh	1451	1461	ν(CC), δ(CH)
			1425sh			1430sh	1430sh	1430s	ν(CC)
						1387	1387	1387m	ν(COO)
1375s,b	1375b	1375b							δ(OH)
			1310	1310	1312	1310sh	1310sh	1316	ν(CO) + ν(CC)
1278vs	1278vs	1281s							ν(CO)
			1280sh	1280sh	1280sh	1277	1278	1275s	ν(COC)
1259vs	1259vs	1258s	1257vs	1257vs	1257vs	1260vs	1259	1261vs	ν(CO)
1226sh	1226sh	1226							δ(OH)
			1210sh			1219	1218	1219	
1200s	1200	1200				1197	1195	1198	δ(OH)
						1180	1181	1180	
						1138	1158	1154	
1103s	1103	1103	1103	1103	1103	1103			δ(CH)
							1077b		ν(PO)
1034	1034	1034	1024	1024	1024	1027			δ(CH)

vs: very strong; s: strong; sh: shoulder; b: broad.

When phosphate was added, competitive adsorption between catechol and phosphate ligands occurred. As shown in Fig. 3c, when pH was decreased from 8.5 to 4.5, the intensity of bands assigned to the adsorbed catechol species (centered at 1480 and 1257 cm^{-1}) decreased, and new bands assigned to adsorbed phosphate species appeared in the range of 1150–1000 cm^{-1}. This is because the favorite adsorption pH for phosphate on iron oxide was in the acidic range and in the basic pH range for catechol. In addition, as can be seen in Fig. 3d, phosphate could displace the pre-adsorbed catechol from the surface at pH 6.5, and there was no interaction between the adsorbed catechol and phosphate surface species.

2.3. Surface speciation during oxidation of catechol

The formation and changes of surface species during the oxidation of catechol were monitored by ATR-FTIR spectroscopy. As can be seen in Fig. 4a and 4b, the spectral intensity increased significantly with time between 1200 and 1600 cm^{-1} after addition of H_2O_2 without phosphate. For 0.2 mmol/L catechol solution (Fig. 4b), all the spectra were still dominated by the bands of adsorbed catechol at 1480 and 1260 cm^{-1}, although the bands were shifted *ca.* 5 cm^{-1} to higher wavenumber, and new bands at 1532, 1430, and 1387 cm^{-1} could be resolved and grew with time. Upon increase of catechol concentration to 1 mmol/L (Fig. 4a), the spectral intensity increased almost 10-fold after 4 hr of reaction compared with the corresponding spectrum of catechol adsorption, and the line shape also changed significantly. By analysis of the second derivative spectra, besides the bands at 1480 and 1260 cm^{-1}, new bands at 1601, 1568, 1532, 1430, 1387, 1349, 1275 and 1219 cm^{-1} were resolved and grew in intensity. The bands at 1532 and 1387 cm^{-1} were assigned to asymmetric and symmetric vibrations of carboxyl groups, indicating the formation of carboxylates upon addition of H_2O_2. The rapid growth of the absorbance at 1267 cm^{-1} in Fig. 4a could be resolved into two bands at 1275 and 1261 cm^{-1} by second derivative spectral analysis. The strong band at 1261 cm^{-1} was assigned to ν(CO) of adsorbed catechol species, and the band at 1275 cm^{-1} was assigned to the combination of an ether C–O–C stretch between aromatic rings and the O–H bending vibration (Dubey et al., 1998; Lana-Villarreal et al., 2005), suggesting the formation of polymeric catechol species during the oxidation. The IR results were consistent with the results from previous work in which the formation of carboxylates, alcohols and dimers of catecholate species, such as 2-furanglycolic acid, 1,2-benzendicarboxylic acid and formic acid, oxalic acid, maleic acid and succinic acid, was identified for the oxidation of catechol by Fe_3O_4–H_2O_2, by GC–MS (Gas Chromatography-Mass Spectrometer), ESI-Q-TOF-MS and ion chromatography analysis (He et al., 2014).

As shown in Fig. 4c, the most striking effect of phosphate in the oxidation process was the rapid increase in the absorbance centered at 1056 cm^{-1}. This spectral feature is similar to the spectra of $FePO_4$ (Guo et al., 2015). Actually, this peak could be resolved into several bands in the wavenumber range of 1150–900 cm^{-1} by second derivative analysis, *viz.* bands at 950, 1001, 1028, 1048, 1063, 1073, 1087, 1097 cm^{-1}. The band in the range of 1019–1033 cm^{-1} could be assigned to symmetric stretching modes of $(PO_4)^{3-}$ tetrahedra in the Q^0 structure (Lu et al., 2015), and the band in the range of 1063–1087 cm^{-1} could be assigned to the stretching vibration of the Fe–O–P bond (Kim et al., 2010). Therefore, the spectral results suggested the formation of iron phosphate precipitation at the surface of catalyst, considering the low solubility product for iron phosphate. In addition, it is also implied that the concentration of iron ions in the mineral-aqueous interface region may increase at the initial stage upon addition of hydrogen peroxide. Accordingly, the reaction of the catalyst with H_2O_2 may cause dissolution of iron atoms from the surface, though the Fe concentration in the solution was rather low. Therefore, the precipitation of iron phosphate may affect the amount of iron atoms taking part in the catalytic decomposition of H_2O_2 and formation of hydroxyl radicals, and then inhibit the catalytic ability of the magnetite surface.

2.4. Effect of phosphate on heterogeneous Fenton reaction mechanism

As shown in Fig. 5, the pH of the solution dropped from 6.5 to below 4 after 1 hr of reaction, regardless of the presence of phosphate ions. The low concentration of phosphate was insufficient to buffer the pH. Meanwhile, the leaching of iron increased with time when phosphate was not added. However, when phosphate was introduced, the concentration of iron increased only in the initial first hour of reaction

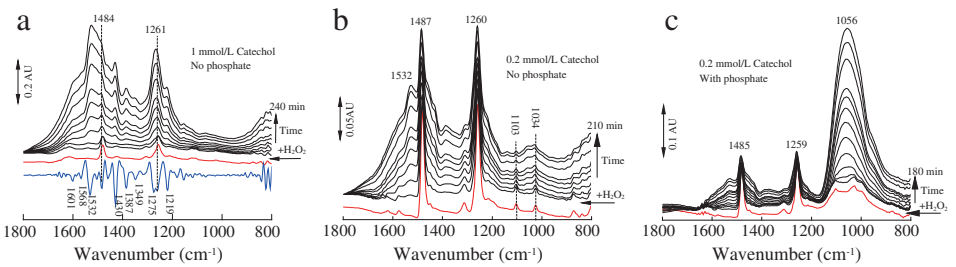

Fig. 4 – *In situ* ATR-FTIR spectra of 1 mmol/L catechol solution at pH 4.5 (a), 0.2 mmol/L catechol solution without phosphate (b) and with phosphate (c) at pH 6.5 in Fe_3O_4–H_2O_2 system. Spectra of pre-adsorbed catechol are shown as red lines, blue line in panel (a) is the second derivative spectrum of 240 min spectrum (the top spectrum in (a)). $[Phosphate]_0$ = 0.05 mmol/L, $[H_2O_2]_0$ = 0.05 mol/L.

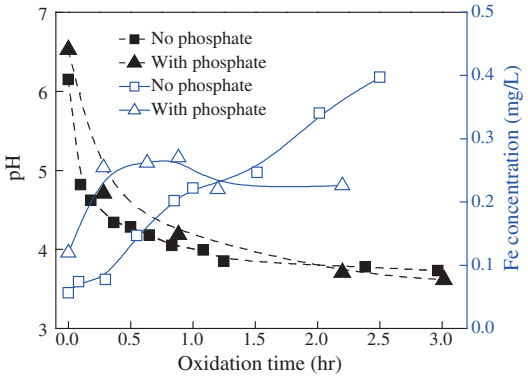

Fig. 5 – Variation of pH (left Y-axis, black symbols) and dissolved Fe concentration (right Y-axis, blue symbols) during the oxidation of catechol catalyzed by MNPs. [Catechol]$_0$ = 1 mmol/L, [H_2O_2]$_0$ = 0.05 mol/L, [$H_2PO_4^-$]$_0$ = 0.1 mmol/L, [MNPs] = 1 g/L, pH$_0$ = 6.5.

and maintained a relatively low level (<0.25 mg/L). The ESR spectra in Fig. 6 shows the typical four-line signal of DMPO-OH ($a_N = a_H$ = 15.0 G), indicating the formation of .OH. Addition of phosphate to the solution and pre-adsorption of phosphate on Fe_3O_4 catalyst both inhibited the production of .OH from H_2O_2 decomposition.

Based on the information outlined above, a possible reaction mechanism of the oxidation of catechol in Fe_3O_4–H_2O_2 heterogeneous system with the presence of phosphate is proposed in Fig. 7. Phosphate could compete with catechol and H_2O_2 for the surface sites of the catalyst, resulting in a reduction of organic removal and H_2O_2 decomposition. Moreover, the formation of iron phosphate species or precipitation on the catalyst surface could reduce the iron leaching, following a restrained homogeneous Fenton catalytic oxidation. Therefore, the removal of DOC was largely restrained by the presence of phosphate, although the consumption of H_2O_2 was significantly reduced at the same time. Before using phosphate as a pH buffer or H_2O_2 stabilizer in a

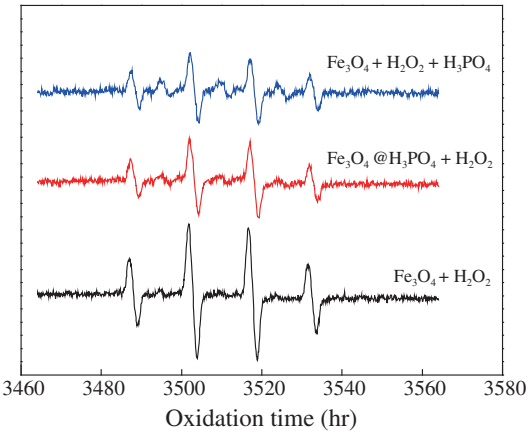

Fig. 6 – ESR spectra of DMPO-OH in aqueous dispersion. Experiments in each graph were conducted under identical instrument parameters.

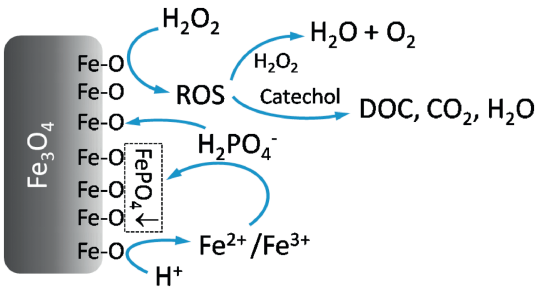

Fig. 7 – Schematic diagram of the inhibition mechanism of phosphate on heterogeneous Fenton reactions.

heterogeneous Fenton system, the possible inhibitory effect of phosphate on the mineralization level of organic pollutants should be fully considered.

3. Conclusions

The effect of phosphate on adsorption and oxidation of catechol in a heterogeneous Fenton system consisting of magnetite nano-particles and H_2O_2 was investigated. The presence of phosphate decreased the removal rate of catechol and the abatement of DOC, as well as the decomposition of H_2O_2. The oxidation and mineralization efficiency were increased slightly due to the decreased consumption of H_2O_2 in the presence of phosphate. At neutral and acidic pH, phosphate could displace the adsorbed catechol from the surface of catalyst and also could compete for surface sites with H_2O_2. *In situ* ATR-FTIR spectra indicated the formation of iron phosphate precipitation at the catalyst surface, considering the low solubility product for iron phosphate. The competition among phosphate, catechol and H_2O_2 for the surface sites of the Fe_3O_4 catalyst contributed to the reduction in both decomposition rate of H_2O_2 and removal of organics. Therefore, the presence of phosphate may affect the amount of iron atoms taking part in the catalytic decomposition of H_2O_2 and formation of hydroxyl radicals. Phosphate ions thus worked as a H_2O_2 stabilizer and oxidation inhibitor in the heterogeneous Fenton reaction at the same time by inhibiting the catalytic ability of Fe_3O_4, due to the strong surface affinity with iron oxide. Before using phosphate as a pH buffer or H_2O_2 stabilizer in a heterogeneous Fenton system, the possible inhibitory effect of phosphate on the actual removal of organic pollutants should be fully considered. The presence of ligands such as phosphate and silicate that tend to form precipitates on the catalyst will inhibit the reactivity of the catalyst. However, when the efficient utilization of H_2O_2 for organic pollutant removal is critical in heterogeneous Fenton oxidation, phosphate could be used as a H_2O_2 stabilizer. In most cases, a pH buffer may not be needed due to the relatively high pH tolerance of the heterogeneous Fenton oxidation.

Acknowledgments

This work was supported by the National Natural Science Foundation of China (Nos. 21107125, 21577160, 51290282, 51221892), the National Basic Research Program (973s) of China

(No. 2011CB933704), and the Hjalmar Lundbom Research Center at Luleå University of Technology.

Appendix A. Supplementary data

Supplementary data associated with this article can be found in online version at doi: http://dx.doi.org/10.1016/j.jes.2015.11.007.

REFERENCES

Duan, F., Yang, Y.Z., Li, Y.P., Cao, H.B., Wang, Y., Zhang, Y., 2014. Heterogeneous Fenton-like degradation of 4-chlorophenol using iron/ordered mesoporous carbon catalyst. J. Environ. Sci. 26 (5), 1171–1179.

Dubey, S., Singh, D., Misra, R.A., 1998. Enzymatic synthesis and various properties of poly(catechol). Enzyme Microb. Technol. 23 (7–8), 432–437.

DuVall, S.H., McCreery, R.L., 2000. Self-catalysis by catechols and quinones during heterogeneous electron transfer at carbon electrodes. J. Am. Chem. Soc. 122 (28), 6759–6764.

Gulley-Stahl, H., Hogan, P.A., Schmidt, W.L., Wall, S.J., Buhrlage, A., Bullen, H.A., 2010. Surface complexation of catechol to metal oxides: an ATR-FTIR, adsorption, and dissolution study. Environ. Sci. Technol. 44 (11), 4116–4121.

Guo, S., Zhang, G., Yu, J.C., 2015. Enhanced photo-Fenton degradation of rhodamine B using graphene oxide-amorphous $FePO_4$ as effective and stable heterogeneous catalyst. J. Colloid Interface Sci. 448, 460–466.

He, J., Yang, X.F., Men, B., Bi, Z., Pu, Y., Wang, D.S., 2014. Heterogeneous Fenton oxidation of catechol and 4-chlorocatechol catalyzed by nano-Fe_3O_4: role of the interface. Chem. Eng. J. 258, 433–441.

Hu, X.B., Liu, B.Z., Deng, Y.H., Chen, H.Z., Luo, S., Sun, C., Yang, P., Yang, S.G., 2011. Adsorption and heterogeneous Fenton degradation of 17 alpha-methyltestosterone on nano Fe_3O_4/MWCNTs in aqueous solution. Appl. Catal. B Environ. 107 (3–4), 274–283.

Hug, S.J., 1997. In situ Fourier transform infrared measurements of sulfate adsorption on hematite in aqueous solutions. J. Colloid Interface Sci. 188 (2), 415–422.

Jolivet, J.P., Tronc, E., 1988. Interfacial electron-transfer in colloidal spinel iron-oxide-conversion of Fe_3O_4-γ-Fe_2O_3 in aqueous-medium. J. Colloid Interface Sci. 125 (2), 688–701.

Kakarla, P.K.C., Watts, R.J., 1997. Depth of Fenton-like oxidation in remediation of surface soil. J. Environ. Eng. 123 (1), 11–17.

Kim, S.W., Ryu, J., Park, C.B., Kang, K., 2010. Carbon nanotube-amorphous $FePO_4$ core-shell nanowires as cathode material for Li ion batteries. Chem. Commun. 46 (39), 7409–7411.

Kummert, R., Stumm, W., 1980. The surface complexation of organic acids on hydrous g-Al_2O_3. J. Colloid Interface Sci. 75 (2), 373–385.

Lana-Villarreal, T., Rodes, A., Perez, J.M., Gomez, R., 2005. A spectroscopic and electrochemical approach to the study of the interactions and photoinduced electron transfer between catechol and anatase nanoparticles in aqueous solution. J. Am. Chem. Soc. 127 (36), 12601–12611.

Li, D.P., Qu, J.H., 2009. The progress of catalytic technologies in water purification: a review. J. Environ. Sci. 21 (6), 713–719.

Lin, S.S., Gurol, M.D., 1998. Catalytic decomposition of hydrogen peroxide on iron oxide: kinetics, mechanism, and implications. Environ. Sci. Technol. 32 (10), 1417–1423.

Lipczynskakochany, E., Sprah, G., Harms, S., 1995. Influence of some groundwater and surface waters constituents on the degradation of 4-chlorophenol by the fenton reaction. Chemosphere 30 (1), 9–20.

Lu, M.W., Wang, F., Liao, Q.L., Chen, K.R., Qin, J.F., Pan, S.Q., 2015. FTIR spectra and thermal properties of TiO_2-doped iron phosphate glasses. J. Mol. Struct. 1081, 187–192.

Martell, A.E., Smith, R.M., 1977. Critical Stability Constant. Plenum Press, New York.

Matta, R., Hanna, K., Kone, T., Chiron, S., 2008. Oxidation of 2,4,6-trinitrotoluene in the presence of different iron-bearing minerals at neutral pH. Chem. Eng. J. 144 (3), 453–458.

Nie, Y.L., Zhang, L.L., Li, Y.Y., Hu, C., 2015. Enhanced Fenton-like degradation of refractory organic compounds by surface complex formation of $LaFeO_3$ and H_2O_2. J. Hazard. Mater. 294, 195–200.

Peak, D., Ford, R.G., Sparks, D.L., 1999. An in situ ATR-FTIR investigation of sulfate bonding mechanisms on goethite. J. Colloid Interface Sci. 218 (1), 289–299.

Persson, P., Nilsson, N., Sjoberg, S., 1996. Structure and bonding of orthophosphate ions at the iron oxide aqueous interface. J. Colloid Interface Sci. 177 (1), 263–275.

Pham, A.L.T., Lee, C., Doyle, F.M., Sedlak, D.L., 2009. A silica-supported iron oxide catalyst capable of activating hydrogen peroxide at neutral pH values. Environ. Sci. Technol. 43 (23), 8930–8935.

Pham, A.L.T., Doyle, F.M., Sedlak, D.L., 2012. Inhibitory effect of dissolved silica on H_2O_2 decomposition by iron(III) and manganese(IV) oxides: implications for H_2O_2-based in situ chemical oxidation. Environ. Sci. Technol. 46 (2), 1055–1062.

Pignatello, J.J., Oliveros, E., MacKay, A., 2006. Advanced oxidation processes for organic contaminant destruction based on the Fenton reaction and related chemistry. Crit. Rev. Environ. Sci. Technol. 36 (1), 1–84.

Rodriguez, E.M., Fernandez, G., Alvarez, P.M., Hernandez, R., Beltran, F.J., 2011. Photocatalytic degradation of organics in water in the presence of iron oxides: effects of pH and light source. Appl. Catal. B Environ. 102 (3–4), 572–583.

Teel, A.L., Warberg, C.R., Atkinson, D.A., Watts, R.J., 2001. Comparison of mineral and soluble iron Fenton's catalysts for the treatment of trichloroethylene. Water Res. 35 (4), 977–984.

Vicente, F., Rosas, J.M., Santos, A., Romero, A., 2011. Improvement soil remediation by using stabilizers and chelating agents in a Fenton-like process. Chem. Eng. J. 172 (2–3), 689–697.

Watts, R.J., Dilly, S.E., 1996. Evaluation of iron catalysts for the Fenton-like remediation of diesel-contaminated soils. J. Hazard. Mater. 51 (1–3), 209–224.

Watts, R.J., Foget, M.K., Kong, S.H., Teel, A.L., 1999. Hydrogen peroxide decomposition in model subsurface systems. J. Hazard. Mater. 69 (2), 229–243.

Watts, R.J., Finn, D.D., Cutler, L.M., Schmidt, J.T., Teel, A.L., 2007. Enhanced stability of hydrogen peroxide in the presence of subsurface solids. J. Contam. Hydrol. 91 (3–4), 312–326.

Xu, L.J., Wang, J.L., 2012. Magnetic nanoscaled Fe_3O_4/CeO_2 composite as an efficient Fenton-like heterogeneous catalyst for degradation of 4-chlorophenol. Environ. Sci. Technol. 46 (18), 10145–10153.

Xue, X.F., Hanna, K., Abdelmoula, M., Deng, N.S., 2009. Adsorption and oxidation of PCP on the surface of magnetite: kinetic experiments and spectroscopic investigations. Appl. Catal. B Environ. 89 (3–4), 432–440.

Yang, X.F., Roonasi, P., Holmgren, A., 2008. A study of sodium silicate in aqueous solution and sorbed by synthetic magnetite using in situ ATR-FTIR spectroscopy. J. Colloid Interface Sci. 328 (1), 41–47.

Yang, Y.L., Yan, W., Jing, C., 2012. Dynamic adsorption of catechol at the goethite/aqueous solution interface: a molecular-scale study. Langmuir 28 (41), 14588–14597.

Zhang, S.X., Zhao, X.L., Niu, H.Y., Shi, Y.L., Cai, Y.Q., Jiang, G.B., 2009. Superparamagnetic Fe_3O_4 nanoparticles as catalysts for the catalytic oxidation of phenolic and aniline compounds. J. Hazard. Mater. 167 (1–3), 560–566.